

Effect of Drying Pretreatment on the Acetylation of Nanofibrillated Cellulose

Vesna Žepič,^a Ida Poljanšek,^{b,*} Primož Oven,^{b,*} Andrijana Sever Škapin,^c and Aleš Hančič^a

The aim of this study was to evaluate the effect of different morphologies of solvent-exchanged (NFC_{SE}), spray-dried (NFC_{SD}), and freeze-dried (NFC_{FD}) nano-fibrillated cellulose on the susceptibility to surface modification with the acetic anhydride/pyridine system. The degree of substitution (DS), morphology, degree of crystallinity (I_{cr}), hydrophobicity, and thermal stability of acetylated products were examined. Acetylated NFC_{SD} and NFC_{FD} had higher DS than acetylated NFC_{SE}, suggesting that drying pre-treatment increased the susceptibility of NFC for acetylation. The morphology of acetylated NFC_{FD} and NFC_{SD} with higher DS was different from unmodified samples, while that of NFC_{SE} was not affected by acetylation. Microspheres of acetylated NFC_{SD} started to dissolve when the highest DS was reached. As opposed to unmodified NFC_{FD}, the nanofibrillar units of acetylated NFC_{FD} became individualised at lower DS. Acetylated samples had lower I_{cr} than the unmodified samples. A significant increase in the contact angle was observed at higher DS of acetylated NFC samples. Acetylation markedly elevated the thermal stability of the acetylated NFC samples.

Keywords: Acetylation; Freeze dried; Hydrophobicity; Nanofibrillated cellulose; Properties; Spray dried

Contact information: a: TECOS, Slovenian Tool and Die Development Centre, Kidričeva 25, SI-3000 Celje, Slovenia; b: University of Ljubljana, Biotechnical Faculty, Department of Wood Science and Technology, Jamnikarjeva 101, SI-1000 Ljubljana, Slovenia; c: Slovenian National Building and Civil Engineering Institute, Dimičeva 12, SI-1000 Ljubljana, Slovenia;

* Corresponding author: ida.poljansek@bf.uni-lj.si; primoz.oven@bf.uni-lj.si

INTRODUCTION

In recent years, increased attention has been directed to the development of sustainable, green, and environmentally friendly materials, a field in which cellulose plays an important role (Miao and Hamad 2013; Rebouillat and Pla 2013). Cellulose is the most abundant natural polymer on earth, having a unique molecular structure and properties (Dufresne 2010). Cellulose is a linear chain composed of β (1 \rightarrow 4) linked D-glucopyranosyl units. Cellulose chains are hydrogen bonded into microfibrils and microfibrillar aggregates, where highly ordered regions alternate with disordered regions (Zugenmaier 2008).

A significant breakthrough in cellulose applicability has been made by the development of efficient procedures for the disintegration of cellulose fibres (Zimmermann *et al.* 2004; Chakraborty *et al.* 2005; Iwamoto *et al.* 2005; Saito *et al.* 2006; Henriksson *et al.* 2007; Pääkkö *et al.* 2007; Chen *et al.* 2011) into the product referred to as microfibrillated cellulose (MFC) (Herrick *et al.* 1983; Turbak *et al.* 1983). MFC may be composed of nanofibrils, fibrillar fines, fibre fragments, and fibres (Chinga-Carrasco 2011), whereas nano-structures represent a main component of MFC (Abdul Khalil *et al.*

2014). In this work, these cellulose portions will be referred to as nanofibrillated cellulose (NFC).

NFC can compete with other synthetic reinforcing agents in terms of strength to weight ratio (Azizi Samir *et al.* 2005; Šturcova *et al.* 2005; Eichhorn *et al.* 2010), whereas its hydrophilic character represents a major obstacle for its use in combination with hydrophobic polymers. With a chemical modification of the NFC surface, its hydrophilicity and a tendency toward hornification can be drastically reduced (Eyholzer *et al.* 2010; Tingaut *et al.* 2010). Acetylation is a commonly used chemical modification procedure for wood (Hill *et al.* 1998) and cellulose fibres (Fengel and Wegner 1984), and was successfully applied to MFC as well (Tingaut *et al.* 2010).

It has been demonstrated that grafting of acetyl moieties on the surface of various cellulose nanomaterial creates a hydrophobic surface (Jonoobi *et al.* 2010; Tingaut *et al.* 2010; Jonoobi *et al.* 2012) and hence reduces water wettability (Jonoobi *et al.* 2010; Lin *et al.* 2011). Grafting also reduces the degree of crystallinity (Hu *et al.* 2011) and the average size of nanofibers (Rodionova *et al.* 2011), and it preserves the nanofibrillar structure (Hu *et al.* 2011; Missoum *et al.* 2012). Acetylation of NFC has been used for various purposes. Rodionova *et al.* (2011) used acetylation to increase the barrier properties of NFC films. Acetylation was also used for hydrophobization of the NFC surface to improve the dispersion of modified NFC in nonpolar PLA solution for production of nanocomposite cast films (Bulota *et al.* 2012). In addition to NFC with plant origins, acetylation was successfully employed for the esterification of bacterial cellulose (Kim *et al.* 2002; Ifuku *et al.* 2007; Lee *et al.* 2011; Berlioz *et al.* 2009) and tunicin cellulose whiskers (Berlioz *et al.* 2009).

In a previous study, the authors investigated a range of properties of nanofibrillated cellulose obtained after different drying techniques (Žepič *et al.* 2014). It was demonstrated that aggregation phenomena are significantly reduced in freeze-dried specimens compared to the powder obtained by spray-drying. That study also showed that re-dispersed freeze-dried NFC had practically the same rheological properties as never-dried NFC. It was also reported that freeze-dried NFC powder retained the initial morphological structure of NFC (Žepič *et al.* 2014).

To the best of our knowledge there has been no study on the influence of different drying methods on the accessibility for acetylation reaction. Although Lee and Bismarck (2012) recently reported the susceptibility towards organic acid esterification of never-dried and freeze-dried bacterial cellulose, the susceptibility towards acetylation of freeze- and spray-dried in comparison with the susceptibility towards acetylation of solvent-exchanged NFC has not yet been explored.

In this study, the susceptibility of solvent-exchanged (SE), freeze-dried (FD), and spray-dried (SD) NFC for a surface modification was examined by employing the acetic anhydride/pyridine system under heterogeneous reaction conditions. In addition, the influence of the catalyst concentration and the reaction time was studied. The degree of substitution, morphology, degree of crystallinity, hydrophobicity, and thermal stability of acetylated products were examined by Fourier transform infrared spectroscopy (FT-IR), field emission scanning electron microscopy (FE-SEM), X-ray powder diffraction analysis (XRPD), measurements of contact angle, and thermogravimetric analysis, respectively.

EXPERIMENTAL

Materials

Nanofibrillated cellulose (NFC) was supplied by the Centre for Biocomposite and Biomaterial Processing, University of Toronto, Canada, as a water suspension with a solid content of 1.6 wt%. The homogenised NFC suspension, obtained through mechanical disintegration of softwood pulp, consisted of cellulose nanofibrils with diameters in the range of 20 to 60 nm. The pure cellulose content in this sample was 91%, the lignin content was less than 0.3%, and the remaining components were primarily hemicelluloses. Acetic anhydride (Ac_2O , $\geq 99\%$), N,N-dimethylformamide (DMF, anhydrous, 99.8%), pyridine (anhydrous, 99.8%), toluene (99.5%), chloroform (anhydrous, $\geq 99\%$, with 0.5-1.0% ethanol as stabiliser), ethanol (96%), and acetone (99.5%) were all purchased from Sigma-Aldrich (Steinheim, Germany). The reagents were used as received without further purification.

Pre-treatment of NFC

An aqueous NFC suspension was solvent-exchanged using five sequential centrifugations and re-dispersion operations at 7830 rpm and 10 °C for 20 min, first into acetone and then into DMF at a final concentration of 1 wt%. In separate experiments, the NFC suspensions were dried using freeze- and spray-drying processes. Prior to freeze drying, the NFC suspension was frozen using liquid nitrogen and then lyophilised (LyoQuest freeze dryer, Telstar) for 72 h. The pressure within the freeze drying system was set to 0.040 mbar, the temperature of the plates to 22 °C, and the temperature of the condenser to -50 °C. The spray drying of the NFC suspension (0.5 wt%) was performed using a Büchi B-290 lab-scale mini-spray-drying unit (Büchi Corporation, Switzerland) with a water evaporating capacity of 1 L h⁻¹ under the following conditions: inlet temperature 160 ± 10 °C, outlet temperature 50 ± 10 °C, spray flow 750 L h⁻¹, aspirator rate 100%, and peristaltic pump 50% (corresponds to approx. 8 mL min⁻¹). The powdery sample was collected from a separation cyclone with a yield of 68% based on the dry matter. The dried forms of NFC were dispersed into DMF at a concentration of 1 wt% using homogenisation (Ultra Turrax T 25 basic, IKA-Werke, Staufen, Germany) and high intensity ultrasonication (Ultrasonic Vibra cell VC500 (Sonics and Materials, USA), 19 mm needle probe tip, 60% output amplitude, for 10 and 5 min, respectively). The DMF/NFC suspensions obtained are hereafter referred to as solvent exchanged (NFC_{SE}), freeze dried (NFC_{FD}), and spray dried (NFC_{SD}) nanofibrillar cellulose.

Heterogeneous Acetylation of NFC

A 100 mL suspension of DMF/NFC (1% based on the dry weight) was mixed with 35 mL (37.8 g; 0.37 mol) of acetic anhydride (Ac_2O). A predetermined amount of pyridine, which served as a catalyst, was added into the beaker and mixed thoroughly with the reaction mixture under slow homogenisation for 10 min. The pre-treated NFC sample was added into a round-bottomed flask equipped with a condenser and a magnetic stirrer. The reaction was performed under a nitrogen flow and kept at the required temperature of 105 ± 5 °C. At the specific reaction intervals of 30, 60, 300, 600, 900, and 1200 min, samples were withdrawn from the reaction mixture. A series of acetylated products, namely ANFC_{SE}, ANFC_{SD}, and ANFC_{FD}, with different degrees of substitution (DS) were obtained. The effect of the pyridine concentration on the extent of acetylation was studied by adding 1% (P1; 0.02 mol), 2% (P2; 0.04 mol), and 3% (P3; 0.06 mol) (v/v) of pyridine.

Acetylated samples treated with different pyridine concentration were marked as ANFCn P1, ANFCn P2, and ANFCn P3, where n indicates the solvent exchanged (SE), spray-dried (SD), and freeze-dried (FD) NFC. At the end of every experiment, the mixture of NFC and chemical reagents was cooled to room temperature and then the acetylation by-products and remaining reagents were removed through five repeated centrifugation and re-dispersion steps with an 800 mL toluene/ethanol/acetone suspension (4/1/1 by v/v/v). The modified samples were dried in a laboratory oven with circulating air at 105 °C for 24 h and stored in desiccators prior to analysis.

Characterization of the Unmodified and Acetylated NFC

Determination of the acetyl content using FT-IR spectroscopy

The infrared spectra of the unmodified and acetylated NFC_{SE} and NFC_{FD} sheets and powder in the case of NFC_{SD} were recorded using a Spectrum One FTIR spectrometer (Perkin Elmer, USA) in attenuated-total-reflection (ATR) mode on a ZnSe crystal. The spectra were collected at a resolution of 4 cm⁻¹, over the range from 650 to 4000 cm⁻¹. A total of 64 scans were used to collect each spectrum. According to Tingaut *et al.* (2010), the peak heights at 1060 cm⁻¹ (H1060) and 1740 cm⁻¹ (H1740) were calculated using baselines constructed between 1500 and 860 cm⁻¹ and between 1790 and 1690 cm⁻¹, respectively. The peak areas at 1740 cm⁻¹ (A1740) and 1370 cm⁻¹ (A1370) were measured using baselines constructed between 1790 and 1690 cm⁻¹ and between 1394 and 1347 cm⁻¹, respectively. The acetyl content of the modified NFCs was calculated from the ratios A1740/ H1060, H1740/ H1060, and A1370/ H1060 (Tingaut *et al.* 2010), and the average values are reported in this study. Bands of FT-IR spectra were assigned according to Tingaut *et al.* (2010), Adebajo and Frost (2004 a, b), and Sun *et al.* (2002). The acetyl content (Ac %) was determined according to Tingaut *et al.* (2010) using FT-IR calibration curves and the degree of substitution (DS) was then calculated using Eq. 1 (Fordyce *et al.* 1946):

$$DS = (3.86 \times Ac(\%)) / (102.4 - Ac(\%)) \quad (1)$$

It needs to be emphasized that Eq. 1 considers all hydroxyl groups in NFC and not just those on the surface.

Field emission scanning electron microscopy (FE-SEM)

The morphology of the samples was observed in secondary electron mode using a field-emission scanning electron microscope (Zeiss ULTRA plus, Germany) with an acceleration voltage (EHT) of 1 and 2 kV and a working distance of 4.7 mm. The 0.5 wt% suspensions of unmodified and acetylated NFCs (NFC_{SE}, NFC_{SD}, NFC_{FD}, and ANFC_{SE}, ANFC_{SD}, ANFC_{FD}) in CHCl₃ were sonicated at room temperature for 3 min using an Ultrasonic Vibra cell VC500 (Sonics and Materials, USA). A droplet of the suspension was deposited on a glass plate and dried for 1 h at room temperature. Samples were coated with a highly conductive film of gold using a BAL-TEC/SCD_500.

Thermogravimetric analysis (TGA)

The thermal stability of unmodified and acetylated NFC samples was determined using a thermogravimetric analyser (Mettler Toledo TGA/SDTA 851e). The samples were heated in a corundum crucible with a diameter of 8 mm from 25 to 500 °C under a dynamic

argon atmosphere (100 mL min⁻¹) and a heating rate of 20 K min⁻¹. The baseline was subtracted in all measurements.

X-ray powder diffraction analysis (XRPD)

X-ray powder diffraction (XRPD) patterns were collected using a Siemens D5000 X-ray powder diffractometer (XRPD) equipped with Cu K $\alpha_{1,2}$ radiation ($\lambda = 1.5418 \text{ \AA}$, 40 kV, and 30 mA), working in reflection mode, from $2\theta = 5^\circ$ to $2\theta = 50^\circ$ with a step size of 0.040° . The unmodified and acetylated NFC_{SE} and NFC_{FD} sheets and the NFC_{SD} powders were uniaxially pressed to form pellets with thicknesses of 1 mm, and their surfaces were analysed. Simulated diffraction patterns of cellulose I β obtained by using Mercury 3.3 software from the Cambridge Crystallographic Data Centre (French 2014) were compared to the experimental patterns.

The internal reference peak height method, developed by Segal and co-workers (1959), was used for comparing the relative differences between the unmodified and acetylated samples. The estimated crystallinity index (I_{cr}) was determined using Eq. 2, where I_{200} ($2\theta = 22.7^\circ$) represents both crystalline and amorphous material, while I_{am} (the minimum between the (200) and (110) peaks, $2\theta = 18^\circ$) represents amorphous material.

$$I_{cr} = \left[\frac{I_{200} - I_{am}}{I_{200}} \right] \times 100 \quad (2)$$

The crystallite size and the number of cellulose chains for both experimental and simulated diffraction patterns were determined by the Scherrer equation (Eq. 3) and by dividing the crystallite size by 3.9 \AA representing the thickness of the cellulose chain (Nishiyama *et al.* 2012; French and Santiago Cintr3n 2013), respectively.

$$\tau = K\lambda / (\beta \cos \theta) \quad (3)$$

In Eq. 3, K is a constant (1.0), λ is the X-ray wavelength, β is the full width at half maximum in radians, and θ is the half of the plotted 2θ value at the position of the studied peak.

Hydrophobicity measurements

Static contact angle measurements were performed at room temperature using a Kr3ss, DSA100 contact angle system. Prior to contact angle measurements, pellets were prepared with a smooth surface and a diameter of 11 mm by pressing the unmodified and acetylated NFC on a hydraulic pressing machine with a force of 10 tons. A droplet of distilled water (vol. $1.5 \mu\text{L}$) was then deposited onto the surface of the pellets and the contact angle was measured after 1 s. Five droplets were deposited on different positions of the sample to reduce the possible influence of the heterogeneity of the surface. The average values of the contact angle measurements are reported.

Determining the residual water content of NFC/DMF suspensions

The water content in the initial DMF/NFCs suspensions was analysed according to the principle of dry-coulometric Karl-Fischer back titration using a Mettler Toledo C30 Coulometer device with a Stromboli sample changer oven (Mettler-Toledo GmbH, Greifensee, Switzerland). The temperature was set to 105°C . The sample was weighed at a precision of 0.1 g and swept with a molecular-sieve dried air stream for approximately 8 min.

RESULTS AND DISCUSSION

FT-IR Spectra of Unmodified and Acetylated NFC

FT-IR spectra for all acetylated NFC samples (Fig. 1) showed three main ester bands at 1740 (carbonyl C=O stretching of ester), 1369 [C-H in -O(C=O)-CH₃], and 1234 cm⁻¹ (C-O stretching of acetyl group). The intensity of these bands increased with increasing reaction time. On the other hand, the intensities of the -OH stretching band at 3337 cm⁻¹ and the -OH in-plane bending bands at 1337 and 1310 cm⁻¹ decreased, which was much more obvious in the cases of ANFC_{FD} and ANFC_{SD}. The absence of typical twin bands of acetic anhydride, which appear in the region from 1840 to 1760 cm⁻¹, indicated that there was no reactant present in acetylated NFCs. The absence of a peak at 1700 cm⁻¹ for a carboxylic group in the spectra of the acetylated samples also indicated that the acetylated products were free of the acetic acid by-product (Sun *et al.* 2002). When comparing the FT-IR spectra of the acetylated NFCs, it was found that both the reaction time and sample pre-treatment had an influence on the DS (Fig. 2). ANFC_{SD} and ANFC_{FD} exhibited pronounced acetylation peaks, particularly at longer reaction times, compared to ANFC_{SE} samples. The observed differences may have been caused by trace water in the reaction mixtures, originating from the possibly incomplete solvent exchange procedure for the NFC_{SE} samples. Another reason for the more pronounced intensities of the -OH groups in the case of ANFC_{SE} can be ascribed to the erosion mechanism of microfibrils (Sassi and Chanzy 1995) caused by acetylation where new -OH groups are exposed on the surface. Sassi and Chanzy (1995) proposed the erosion mechanism where a part of a cellulose chain located at the surface is sufficiently acetylated. It then becomes soluble in the acetylating medium and is lifted from the surface of the crystalline lattice.

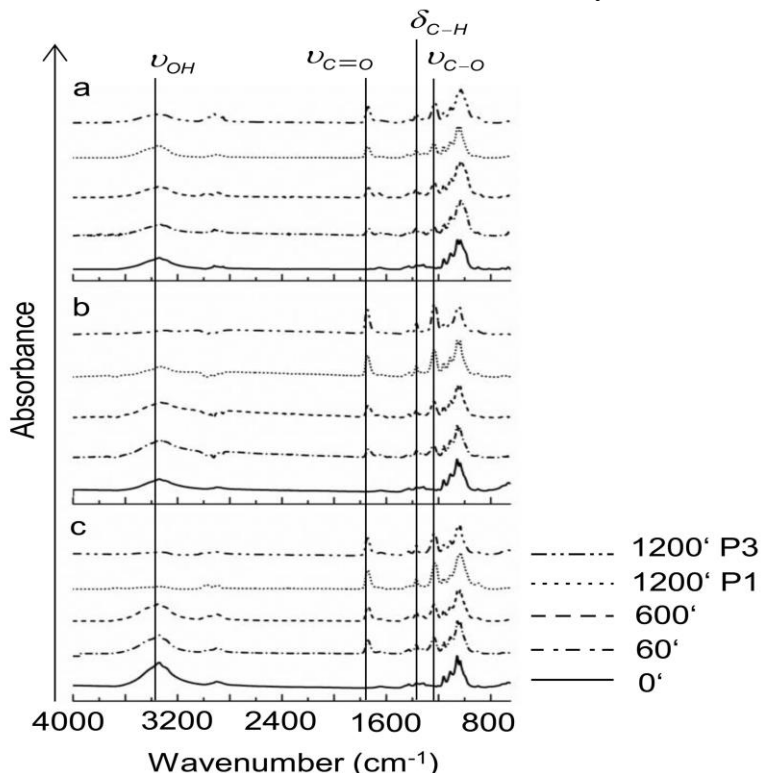


Fig. 1. FT-IR spectra of the unmodified and acetylated (a) NFC_{SE}, (b) NFC_{SD}, and (c) NFC_{FD} obtained after different reaction times: 0 (unmodified), 60, 600, and 1200 min. Pyridine concentration of 1 vol.% and 3 vol.% at 1200 min is labelled by P1 and P3, respectively.

Degree of Substitution for Acetylated NFC

The catalyst concentrations, the values of DS, and the residual water contents for each acetylated product are listed in Table 1. The esterification reaction in the presence of low catalyst concentrations (1 vol.%) gave DS values in the range of 0.48, 0.85, and 1.00 for ANFC_{SE}, ANFC_{SD}, and ANFC_{FD}, respectively (Table 1). When the same reaction was carried out in the presence of higher catalytic amounts, 2 vol.% and 3 vol.%, higher values of DS were obtained for ANFC_{SE} and ANFC_{SD} (Table 1). According to Sassi and Chanzy (1995), the acetylation reaction starts within the amorphous region and in a second step the acetylation occurs in the crystallites as an erosion mechanism. It was assumed that other available hydroxyl groups, which might be located deeper in the nanofibrillar structures, were involved in the reaction as well, especially at the highest pyridine concentration for NFC_{SD}. Higher pyridine concentration had no impact on the DS for ANFC_{FD}.

Table 1. Degree of Substitution of the Acetylated NFC_{SE}, NFC_{SD}, and NFC_{FD} Samples at Different Catalyst Concentration and Reaction Time 1200 min. *

Catalysts concentration	Degree of substitution		
	ANFC _{SE}	ANFC _{SD}	ANFC _{FD}
P1 (1 vol%)	0.48 ± 0.014	0.85 ± 0.025	1.00 ± 0.104
P2 (2 vol%)	0.75 ± 0.038	1.36 ± 0.051	0.98 ± 0.124
P3 (3 vol%)	0.90 ± 0.006	1.53 ± 0.016	0.93 ± 0.081
Residual water content (%)	1.31 ± 0.096	0.79 ± 0.193	0.47 ± 0.060

* Residual water content is given for NFC/DMF samples.

Figure 2 shows the DS as a function of the reaction time for NFC_{SE}, NFC_{SD}, and NFC_{FD}. For all three materials, the DS increased with reaction time (Fig. 2).

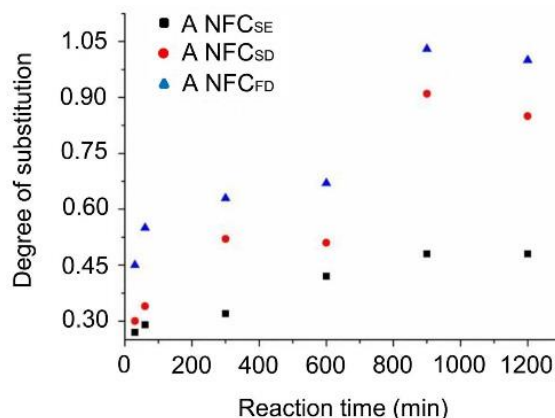


Fig. 2. The degree of substitution as a function of reaction time for the acetylated NFC_{SE}, NFC_{SD}, and NFC_{FD} at 1 vol.% of pyridine

The DS values increased rapidly during the first hour of acetylation. Thereafter, the DS increased gradually until 900 min, where an additional rise in the DS was observed for all acetylated NFC samples, regardless of the applied pre-treatment. This was pronounced

for ANFC_{SD} and ANFC_{FD}, where DS was higher than for the solvent exchanged ANFCs, suggesting that drying increased the susceptibility of NFC for acetylation. It is assumed that the drying pre-treatment significantly increased the swelling ability of the cellulose and the diffusion rate of the acetic anhydride and pyridine, which was evaluated from the measurements of the size of the average diameter of the nanofibrils (Fig. 3).

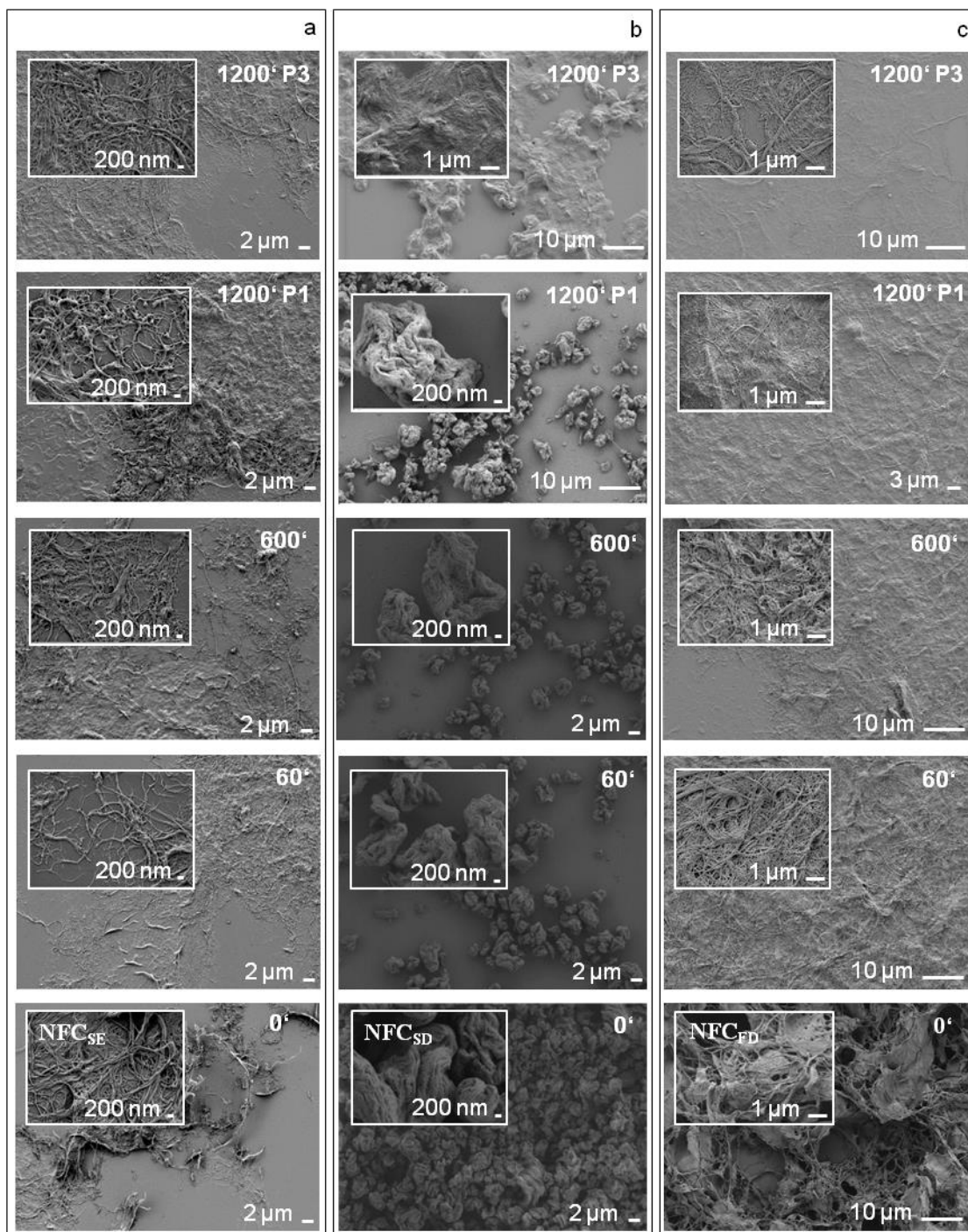


Fig. 3. FE-SEM images of unmodified (0 min) and acetylated (a) NFC_{SE}, (b) NFC_{SD}, and (c) NFC_{FD} at selected reaction times are organized in columns. Pyridine concentration of 1 vol.% and 3 vol.% at 1200 min is labelled by P1 and P3, respectively.

The higher initial reaction rate of acetylation for NFC_{FD} was ascribed to the lower water content in the initial material. The lower the water content, the higher the reaction rate at the beginning. After 900 min, the modified samples started to reach a constant value (equilibrium). Thereafter, a slight decrease in the DS was observed in some cases. This may be ascribed to the reversibility of the esterification reaction. Although longer reaction times (72 h) were also investigated in the preliminary study, no further increase in DS was observed. Because longer reaction times would result in the hydrolysis of the ester groups and/or the decomposition of the cellulose backbones (Satgé *et al.* 2002; Li *et al.* 2009a,b; Hu *et al.* 2011), the reaction time of 1200 min was selected to test the influence of a higher pyridine concentration. Pyridine is reported to be highly effective at accelerating the rate of the reaction of acetic anhydride with the accessible, reactive hydroxyl sites on the NFC surface (Hill *et al.* 2000; Hill and Papadopoulos 2002; Li *et al.* 2011) because it not only swells the cellulose fibres (Jonoobi *et al.* 2012; Sun *et al.* 2002) but it also catalyses the reaction via nucleophilic mediated catalysis (Satchell 1963; Hill *et al.* 2000; Tosh *et al.* 2000; Sun *et al.* 2001).

It was assumed that the DS of around 1 was a limiting value for the reaction of acetylation; beyond that the erosion mechanism started to prevail and new -OH groups were exposed on the surface. In the case of NFC_{SE}, the erosion mechanism was supposed to start when 3 vol% of pyridine was used. This assumption was supported by the fibril dimensions (Fig. 3). On the other hand, no reduction in fibril size of NFC_{FD} was seen. This can be ascribed to the pre-treatment procedure in which new hydrogen bonds are formed to some extent during freeze drying. It seems that these bonds were relatively strong and, under acetylation conditions, it was impossible to cleave them. As a result, higher amounts of the catalyst had no major effect on the acetylation reaction of NFC_{FD}. This is illustrated in Fig. 1c, showing that the peak intensity of the hydroxyl stretching vibration region of the infrared spectra (3337 cm^{-1}) for ANFC_{FD} at 1200 min was low when the catalyst concentration was 1 vol.%. It is therefore possible that all accessible hydroxyl groups of the NFC_{FD} were acetylated to the final value already at this pyridine concentration. Another explanation can be found in the residual water content of the NFC/DMF samples. Beside catalytic function, pyridine acted as water scavenger in this reaction. The higher the content of residual water, the higher content of pyridine was needed to reach higher DS and vice versa. The acetylation of cellulose is a reversible reaction; thus, the residual water content of the NFC/DMF samples inhibited the course of the reaction. If water is removed from the system, the equilibrium of the reaction will shift towards the ester production (Lee and Bismarck 2012). Another reason why the residual water content in the reaction mixture should be as low as possible is that the interaction of water with the cellulosic -OH groups may hinder the access of the acetic anhydride, resulting in a lower DS of acetylated products. Additionally, residual water can decompose the anhydride to acetic acid with lower reactivity.

The highest values of residual water content were observed in the NFC_{SE} samples, while the NFC samples pre-treated with drying had a significantly lower amount of free water. Considering these results, the efficiency of water removal was much greater through the drying pre-treatment methods than the solvent exchange method. The latter requires the exchange of solvents using several repeated centrifugation and re-dispersions cycles to eliminate all the trace of free water, which makes this technique time consuming. This feature shows that traces of water remaining in the NFC_{SE}/DMF suspension affected the acetylation procedure and decreased the DS obtained for the acetylated products. Our results indicate that the drying pre-treatment seems to be an important factor in the

acetylation process because the initial rate of acetylation decreases as the water content increases (Fig. 2).

Morphology of the Acetylated NFC

The morphology of the unmodified and acetylated NFC samples after selected reaction times and at 1200 min by using 1 vol.% or 3 vol.% pyridine (Table 1) is shown in Fig. 3. The morphology of the NFC_{SE} sample had a web-like structure that is typical of NFCs, as demonstrated by Žepič *et al.* (2014). Despite acetylation at prolonged reaction times, this morphology was preserved. Although the size of the nanofibrils was very variable, the average diameter could be evaluated from 40 ± 8 nm for unmodified NFC_{SE} to 46 ± 22 nm for ANFC_{SE} at P1 (DS = 0.48) and 29 ± 10 nm for ANFC_{SE} at P3 (DS = 0.90). Hence, when NFC_{SE} was treated with the highest catalyst concentration, 3 vol.%, its size decreased, although the DS value increased significantly. The decrease in the size of the nanofibrils at higher concentrations of pyridine can be ascribed to the erosion mechanism.

The NFC_{SD} appeared in the form of microspheres with a folded surface (Fig. 3) as a result of the applied spray drying evaporation process (Žepič *et al.* 2014). The morphology of ANFC_{SD} did not change to an obvious extent at reaction times from 60 to 1200 min and 1 vol.% of pyridine concentration. This result indicated that the spherical shape of the particles remained preserved after moderate surface modification when using the 1 vol.% of catalysts. Conversely, by increasing the pyridine concentration (3 vol.%), the DS increased up to 1.53 and the morphology of the sample changed significantly. Microspheres could not be identified and the general appearance of the material was blurry. This may have resulted from a partial solubilisation of the cellulose derivatives in the low-polarity organic solvent (*i.e.*, CHCl₃).

The unmodified NFC_{FD} sample had a highly porous structure defined with nanofibrillar networks, where closer examination revealed that the fibrils were severely aggregated. The fibrils detected in the unmodified NFC_{FD} sample were 43 ± 16 nm in diameter and the pores varied in size from hundreds of nanometres to several microns. In contrast to unmodified NFC_{FD}, the acetylated nanofibrillar units became visible already after 60 min of reaction. Longer reaction times did not essentially change the morphology of ANFC_{FD}. The diameters of the acetylated fibrils (ANFC_{FD}) treated with 1 and 3 vol.% of catalysts were estimated to be 46 ± 17 nm and 48 ± 11 nm, respectively, in the thinnest dimension. The increase in size of acetylated nanofibrills was ascribed to the introduction of bulky acetyl groups to the inside of the nanofibrills. Another reason was attributed to the hydrophobization of the NFC surface which improves the swelling of modified NFC in nonpolar solvent.

We speculate that the mechanism of acetylation in the pretreated NFC_{FD} might be the same as in the case of solvent-exchanged NFC. It was assumed that acetylation reaction proceed through erosion mechanism. This assumption is supported by the results of the morphology as well as the results from FTIR spectroscopy. In the case of NFC_{SD} it is difficult to speculate on the mechanism of acetylation due to the complex morphology of the sample.

X-ray Diffraction Patterns of Acetylated NFC

Figure 4 shows the XRPD patterns for unmodified and ANFC_{SE}, ANFC_{SD}, and ANFC_{FD} using a pyridine concentration of 1 vol.% (P1) or 3 vol.% (P3). Diffraction patterns for cellulose I β with different peak widths at half height simulated from the Mercury program are also presented in Fig. 4.

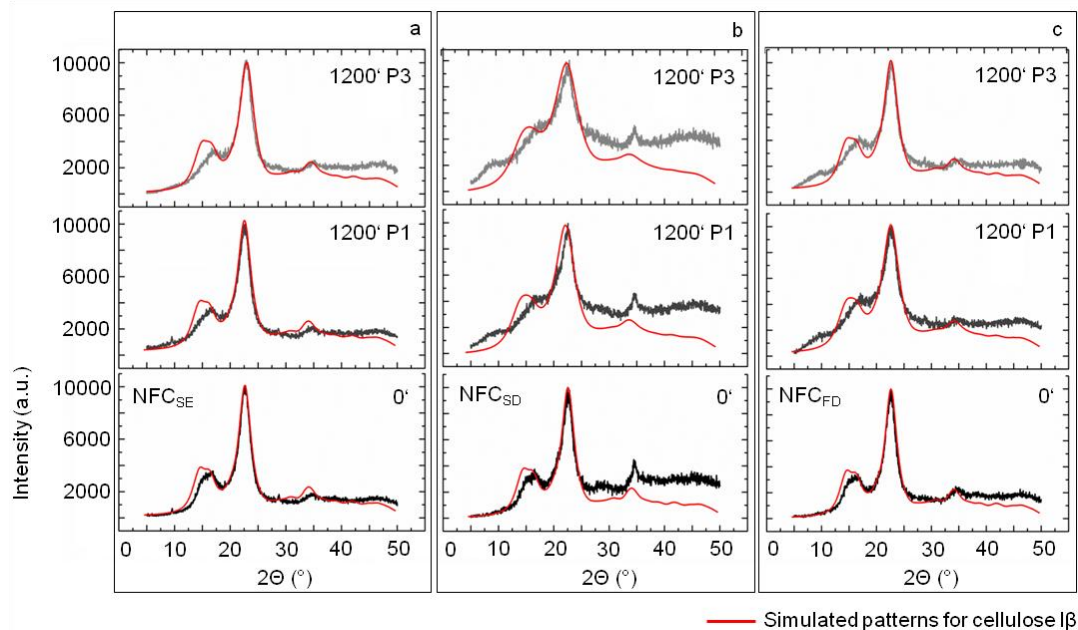


Fig. 4. The experimental and simulated XRPD patterns of unmodified (0 min) and acetylated (a) NFC_{SE}, (b) NFC_{SD}, and (c) NFC_{FD}. Pyridine concentration of 1 vol.% and 3 vol.% at 1200 min is labelled by P1 and P3, respectively.

Three principal diffraction peaks at 2θ angles between 14.5° and 17.5° [(1-10) and (110)], 22.7° (200), and 34.5° (004) (Fig. 4), were assigned to the typical reflection planes of cellulose I β (Freire *et al.* 2006; Maneerung *et al.* 2008; Liu *et al.* 2010; French 2014) and were defined for all unmodified NFC samples, irrespective of the solvent exchanging or drying pre-treatment. It was not possible to distinguish between the diffraction peaks at 14.5° and 17.5° 2θ with Miller indices (1-10) and (110) for acetylated NFC samples. The intensity of the (012) and (102) at 20.3° and 20.6° 2θ peaks was reduced or absent. A possible explanation for this could be the partially oriented powder which was caused by the sample preparation method where pressed pellets were used (French and Santiago Cintr3n 2013). Additionally, from the XRPD of the dried and acetylated NFC samples (Fig. 4b and c), a broad reflection peak was observed at approximately 8° and cited (Kim *et al.* 2002; Tingaut *et al.* 2010; Hu *et al.* 2011) as the principal characteristic of semi-crystalline acetylated derivative cellulose. The position of this peak indicated the presence of cellulose triacetate moieties on the surface of nanofibrils (Kim *et al.* 2002; Tingaut *et al.* 2010; Hu *et al.* 2011), which was confirmed with the calculation of the diffraction pattern for cellulose I β , where no peak at 8° 2θ was observed.

The diffraction patterns calculated from cellulose I β structure were used to simulate the experimental data of unmodified and acetylated NFC_{SE}, NFC_{SD}, and NFC_{FD} samples (French 2014) and the results are presented in Table 2 and Fig. 4 (French and Santiago Cintr3n 2013; Nishiyama *et al.* 2012; French 2014).

The degree of crystallinity (I_{cr}) was found to be in the same range for all untreated forms of NFC. For all acetylated NFC samples, a lower I_{cr} was observed than in the original samples. This was a consequence of the substitution of the hydroxyl groups with acetyl groups, which resulted in the reduction of the hydrogen bond density between the cellulose molecules, partially destroying the crystalline structure of the fibrillar cellulose (Yin *et al.* 2007; Lee and Bismarck 2012). Another reason for the lower I_{cr} of the acetylated NFC

samples could be the reduction of the crystallite size. Calculations supported a model that describes the size of the crystal of the unmodified sample in terms of the number of chains as 9x9 with 32 molecules on the surface of the crystal and with 49 in the interior. The diffraction patterns of the ANFC_{SE} samples seemed to almost agree with the untreated sample, indicating that the original crystalline structure was mostly preserved, as the modification only affected the nanofibrillar surface (Lee *et al.* 2011). A slight decrease was observed in the I_{cr} values, crystallite size, and number of chains for ANFC_{SE} due to the varying catalyst concentration, even though the degree of substitution (DS) increased significantly. It seemed that the crystallite size and I_{cr} of the ANFC_{SE} did not change much until the degree of substitution reached DS=1. This was another indication for the erosion mechanism of acetylation at higher pyridine concentrations for the sample NFC_{SE}.

Conversely, the XRPD patterns of ANFC_{SD} showed a significant reduction in the intensities of all the diffraction planes. The I_{cr} dropped from 77% to 62% and 57% for ANFC_{SD} treated with 1 vol.% and 3 vol.% of the catalysts concentration, respectively, which was an indication that the cellulose lost its crystal structure and crystallite size decreased due to the partial solubility of the sample at higher DS. These results may support the presumption that the acetylation proceeds from the surface to the core of each nanofibrillar unit, and the crystal structure of the ANFC_{SD} changed with the increase of the acetyl DS, similar to the cases reported in previous publications (Sassi *et al.* 2000; Hu *et al.* 2011; Lee and Bismarck 2012). This effect was consistent with the FE-SEM results for ANFC_{SD}.

The I_{cr} value of ANFC_{FD} treated with 1 vol.% pyridine dropped from 78% to 61% and crystallite size from 35 to 25 Å, indicating that the acetylation started at the amorphous regions and proceeded progressively to the crystalline regions. This is the most likely reason for the size reduction of crystallites which coincides with the ICR value. This process does not affect the dimensions of the nanofibril, as was observed by SEM. For ANFC_{FD} treated with 3 vol.% pyridine, a slightly higher I_{cr} (66%) was determined, compared to the sample acetylated under moderate reaction conditions, which was in agreement with DS (Table 1, Table 2).

Water Contact Angle of Acetylated NFC

Table 3 shows contact angles as a function of acetylation reaction time in comparison to unmodified NFC samples. Contact angles of the initial unmodified dried material, NFC_{SE}, NFC_{FD}, and NFC_{SD} were smaller than that of acetylated samples but differed significantly among each other. A significant increase in the contact angle was observed after acetylation, indicating that surface modification induced changes in the surface polarity of the fibrillated cellulose. For all three samples the contact angle increased with the increasing degree of acetylation (Table 3). The acetylation of NFC_{SE} gradually increased the values of the water contact angles from 51.9° to 63.6° as the DS increased with increasing reaction times with 1 vol.% of catalyst. The increased catalysts concentration (3 vol.%) had a small effect on contact angle comparing to 1vol.% of pyridine at 1200 min of reaction time (Table 3).

The contact angle of ANFC_{SD} increased gradually with longer reaction times when using the catalyst at 1 vol.%. ANFC_{SD} synthesized with the higher amount of pyridine (3 vol.%) reached the highest DS, but the contact angle increased only minimally, which is another proof that the acetylation proceeds from the surface to the core of each nanofibrillar unit.

Table 2. Peak Widths at Half Maximum Height (pwhm), Crystallite Size, Minimum Intensity, and Segal ICR

	NFC SE			NFC SD			NFC FD		
	0'	1200' P1	1200' P3	0'	1200' P1	1200' P3	0'	1200' P1	1200' P3
Cellulose I β *									
τ (crystallite size) (Å)	34.7	32.2	30.1	33.3	22.5	18.0	35.3	25.7	28.2
Number of chains	8.88	8.25	7.70	8.55	5.77	4.62	9.06	6.60	7.22
Input pwhm (°)	2.6	2.8	3.0	2.7	4.0	5.0	2.55	3.5	3.2
Minimum intensity	2031	2271	2511	2162	3690	4760	1987	3100	2751
2 θ at min (°)	18.77	18.77	18.77	18.77	18.62	18.25	18.77	16.67	18.77
Nanofibrillated Cellulose**									
τ (crystallite size) (Å)	34.66	30.99	30.05	32.18	19.85	13.55	35.46	21.14	26.66
Number of chains	8.88	7.95	7.70	8.25	5.09	3.47	9.09	5.42	6.84
Measured pwhm (°)	2.6	2.9	3.0	2.8	4.5	6.7	2.5	4.2	3.4
Minimum intensity	2338	2754	2720	2301	3764	4341	2172	3890	3342
2 θ at min (°)	17.96	18.00	18.00	17.88	17.84	16.88	17.84	17.88	17.60
I_{CR} (%)	76.76	72.45	73.32	76.53	62.19	56.66	78.18	61.13	66.41

* From the predicted models in Mercury program

** Measured values from samples used in the present study

Table 3. Mean Values of the Static Contact Angles for Unmodified and Acetylated NFC_{SE}, NFC_{SD}, and NFC_{FD}. *

Sample	Water contact angle (°) at 1s				
	0'	60'	600'	1200' P1	1200' P3
NFC _{SE}	51.9 ± 3.2	58.1 ± 2.3	62.8 ± 3.8	63.6 ± 3.6	66.4 ± 2.4
NFC _{SD}	39.9 ± 8.4	43.9 ± 5.8	58.3 ± 2.9	65.8 ± 2.8	68.2 ± 0.5
NFC _{FD}	44.7 ± 1.8	62.8 ± 1.5	68.7 ± 3.9	72.9 ± 4.4	72.8 ± 2.6

* Pyridine concentration of 1 vol.% and 3 vol.% at 1200 min is labelled by P1 and P3, respectively.

In the case of the ANFC_{FD} treated with a catalyst concentration of 1 vol.%, the contact angle values progressively increased from 44.7° to 72.9° as the DS increased. Moreover, the contact angle values remained almost constant for the acetylated samples treated with higher catalyst concentrations and fixed reaction time, which is in agreement with DS.

Different contact angles of unmodified and acetylated NFC can be attributed to the physical properties of the surface, namely the contact angle of cellulose pellets/films exhibited a higher contact angle while powder pellets had smaller contact angles. The maximum contact angle was achieved for acetylated NFC_{FD}, owing to the high degree of acetylation as well as the physical properties of the sample surface. Sample NFC_{SE} was in the form of films that were stacked one upon another and pressed. The contact angle of this sample was the highest. The lowest contact angle for the initial sample was measured for NFC_{SD} because the initial sample was a compressed powder. The value of the contact angle for the initial compressed sample of NFC_{FD} was in between. We are aware that contact angles of unmodified NFC are rather high for highly hydrophilic materials; this could be attributed to passivation of the cellulose surface (Johansson *et al.* 2011) and on the other hand to the procedure for sample preparation.

Thermal Properties of Acetylated NFC

The thermal properties of unmodified and acetylated NFC_{SE}, NFC_{SD}, and NFC_{FD} samples are illustrated in Fig. 5, where the 5 wt.% weight loss temperatures (T_{5wt%}) are listed.

The TGA curves for unmodified and acetylated NFC were similar and can be divided into three stages. During the initial stage from room temperature to 120 °C, the water and other residue solvent vaporised. From 220 to 390 °C, the crystalline region started to degrade. From 390 to 500 °C, the crystalline region was already completely destroyed, and the cellulose decomposed into monomers of β–glucopyranose, which could be further decomposed into free radicals (Antal and Varhegyi 1995; Yang *et al.* 2008; Hu *et al.* 2011). As shown in Fig. 5a, the onset of the thermal degradation started at 242 °C for the unmodified NFC_{SE} and was systematically shifted to higher temperatures for the acetylated samples treated with a catalyst concentration of 1 vol.%. The T_{5wt%} of ANFC_{SE} increased gradually with reaction time under constant catalyst concentration. However, a lower degradation temperature, 290 °C, was observed for ANFC_{SE} treated with a catalyst concentration of 3 vol.%, even though the highest DS was found in this sample (0.90). For dried, unmodified, and acetylated NFC samples, a similar trend was observed for the evolution of the thermal decomposition with increasing DS values. The onset of thermal degradation was considered to start at 290 °C and 287 °C for the unmodified NFC_{SD} and

NFC_{FD} samples, respectively, while the ANFC_{SD} and ANFC_{FD} samples treated with a catalyst concentration of 3 vol.% started to decompose at 322 °C and 319 °C, respectively. In other words, the decomposition temperature of ANFC_{SD} and ANFC_{FD} was approximately 32 °C higher than that of unmodified samples, which can be attributed to the replacement of hydroxyl groups with the more stable acetyl groups (Hu *et al.* 2011). This result proved that acetylation markedly elevated the thermal stability of the drying pre-treated NFC.

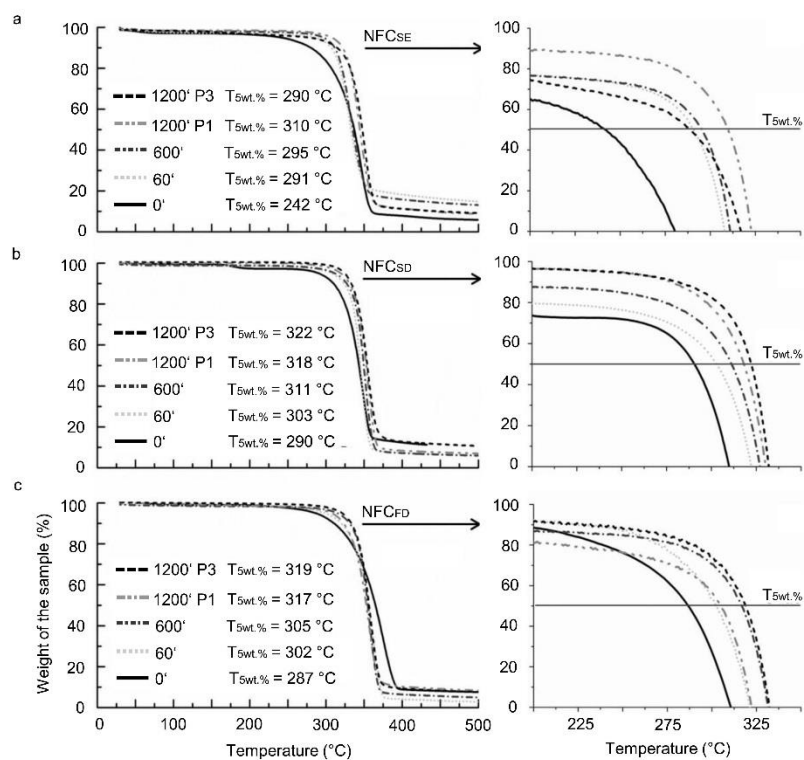


Fig. 5. Thermograms of unmodified (0 min) and acetylated NFC_{SE} (a), NFC_{SD} (b), and NFC_{FD} (c) after selected reaction times. Pyridine concentration of 1 vol.% and 3 vol.% at 1200 min is labelled by P1 and P3, respectively.

CONCLUSIONS

1. The results showed that the degree of acetylation of the freeze- and spray-dried NFC was higher than for the solvent exchanged NFC samples, suggesting that the application of different drying pre-treatments improved susceptibility of dried NFC for acetylation modification.
2. These observations further indicated that the all properties of acetylated NFC investigated in this work depended on the morphology of the starting material obtained after different drying techniques. Maximal degree of substitution at which the morphology of unmodified samples remained preserved was at around 0.9 and 1.0 for acetylated NFC_{SD} and NFC_{FD}.

3. NFC_{FD} was the most appropriate starting (initial) material for acetylation as the achieved degree of substitution was the highest and the morphology and the crystallinity were satisfactorily preserved.
4. The lower residual water content of NFC_{FD} enabled the acetylation reaction to proceed faster and the achievement of the same or even higher DS was obtained using less reagents and less aromatic pyridine catalyst. The process of acetylation in these conditions was much more economic, eco-friendly, and less time consuming.

ACKNOWLEDGMENTS

The authors wish to gratefully acknowledge the Ministry of Higher Education, Science and Technology of the Republic of Slovenia, within the Programs P4-0015. This work was also co-supported by the European Union, European Social Fund, whose contribution is fully recognized.

REFERENCES CITED

- Abdul Khalil, H. P. S., Davoudpour, Y., Nazrul Islam, M. D., Asniza Mustapha Sudesh, K., Dungani, R., and Jawaid, M. (2014). "Production and modification of nanofibrillated cellulose using various mechanical processes: A review," *Carbohydrate Polymers* 99, 649-665. DOI: 10.1016/j.carbpol.2013.08.069
- Adebajo, M. O., and Frost, R. L. (2004a). "Acetylation of raw cotton for oil spill cleanup application: an FTIR and ¹³C MAS NMR spectroscopic investigation," *Spectrochimica Acta, Part A: Molecular and Biomolecular Spectroscopy* 60(10), 2315-2321. DOI: 10.1016/j.saa.2003.12.005
- Adebajo, M. O., and Frost, R. L. (2004b). "Infrared and ¹³C MAS nuclear magnetic resonance spectroscopic study of acetylation of cotton," *Spectrochimica Acta, Part A: Molecular and Biomolecular Spectroscopy* 60(1-2), 449-453. DOI: 10.1016/S1386-1425(03)00249-X
- Antal, M. J., and Varhegyi, G. (1995). "Cellulose pyrolysis kinetics: The current state of knowledge," *Industrial and Engineering Chemistry Research* 34, 703-717. DOI: 10.1021/ie00042a001
- Azizi Samir, M.A.S., Alloin, F., and Dufresne, A. (2005). "Review of recent research into cellulosic whiskers, their properties and their application in nanocomposite field," *Biomacromolecules* 6(2), 612-626. DOI: 10.1021/bm0493685
- Berlioz, S., Molina-Boisseau, S., Nishiyama, Y., and Heux, L. (2009). "Gas-phase surface esterification of cellulose microfibrils and whiskers," *Biomacromolecules* 10, 2144-2151. DOI: 10.1021/bm900319k
- Bulota, M., Kreitsmann, K., Hughes, M., and Paltakari, J. (2012). "Acetylated microfibrillated cellulose as a toughening agent in poly(lactic acid)," *Journal of Applied Polymer Science* 126, 448-457. DOI: 10.1002/app.36787
- Chakraborty, A., Sain, M., and Kortschot, M. (2005). "Cellulose microfibrils: A novel method of preparation using high shear refining and cryocrushing," *Holzforschung* 59, 102-107. DOI: 10.1515/hf.2005.016

- Chen, W., Yu, H., Liu, Y., Hai, Y., Zhang, M., and Chen, P. (2011). "Isolation and characterization of cellulose nanofibers from four plant cellulose fibers using a chemical-ultrasonic process," *Cellulose* 18, 433-442. DOI: 10.1007/s10570-011-9497
- Chinga-Carrasco, G. (2011). "Cellulose fibers, nanofibrils and microfibrils: The morphological sequence of MFC components from a plant physiology and fibre technology point of view," *Nanoscale Research Letter* 6, 417. DOI: 10.1186/1556-276x-6-417
- Dufresne, A. (2010). "Processing of polymer nanocomposites reinforced with polysaccharide nanocrystals," *Molecules* 15(6), 4111-4128. DOI: 10.3390/molecules15064111
- Eichhorn, S. J., Baillie, C. A., Zafeiropoulos, N., Mwaikambo, L. Y., Ansell, M. P., Dufresne, A., Entwistle, K. M., Herrera-Franco, P., Escamilla, G. C., Groom, L., Hughes, M., Hill, C., Rials, T. G., and Wild, P. M. (2010). "Review: Current international research into cellulosic fibres and composites," *Journal of Materials Science* 36(9), 2107-2131. DOI: 10.1023/A:1017512029696
- Eyholzer, C., Bordeanu, N., Lopez-Suevos, F., Rentsch, D., Zimmermann, T., and Oksman, K. (2010). "Preparation and characterization of water-redispersible nanofibrillated cellulose in powder form," *Cellulose* 17(1), 19-30. DOI: 10.1007/s10570-009-9372-3
- Fengel, D., and Wegener, G. (1984). *Wood: Chemistry, Ultrastructure, Reactions*, Walter de Gruyter, Berlin, New York. DOI: 10.1515/9783110839654
- Fordyce, C. R., Genung, L. B., and Pile, M. A. (1946). "Composition of cellulose esters, use of equations and nomographs," *Ind. Eng. Chem., Anal. Ed.* 18, 547-550. DOI: 10.1021/i560157a008
- Freire, C. S. R., Silvestre, A. J. D., Neto, C. P., Belgacem, M. N., and Gandini, A. (2006). "Controlled heterogeneous modification of cellulose fibers with fatty acids: Effect of reaction conditions on the extent of esterification and fiber properties," *J. Appl. Polym. Sci.* 100(2), 1093-1102. DOI: 10.1002/app.23454
- French, A.D. (2014). "Idealized powder diffraction patterns for cellulose polymorphs," *Cellulose* 21, 885-896. DOI: 10.1007/s10570-013-0030-4
- French, A.D., and Santiago Cintrón, M. (2013). "Cellulose polymorphy, crystallite size, and the Segal crystallinity index," *Cellulose* 20, 583-588. DOI: 10.1007/s10570-012-9833-y
- Henriksson, M., Henriksson, G., Berglund, L. A., and Lindstrom, T. (2007). "An environmentally friendly method for enzyme-assisted preparation of microfibrillated cellulose (MFC) nanofibers," *Eur. Polym. J.* 43, 3434-3441. DOI: 10.1016/j.eurpolymj.2007.05.038
- Herrick, F. W., Casebier, R. L., Hamilton, J. K., and Sandberg, K. R. (1983). "Microfibrillated cellulose: morphology and accessibility," *J. Appl. Polym. Sci. Appl. Polym. Symp.* 3, 797-813.
- Hill, C. A. S., Cetin, N. S., and Ozmen, Z. (2000). "Potential catalysts for the acetylation of wood," *Holzforschung* 54, 269-272. DOI: 10.1515/hf.2000.045
- Hill, C. A. S., Jones, D., Strickland, G., and Cetin, N. S. (1998). "Kinetic and mechanistic aspects of the acetylation of wood with acetic anhydride," *Holzforschung* 52, 623-629. DOI: 10.1515/hfsg.1998.52.6.623
- Hill, C. A. S., and Papadopoulus, A. N. (2002). "The pyridine-catalysed acetylation of pine sapwood and phenolic model compounds with carboxylic acid anhydrides.

- Determination of activation energies and entropy of activation,” *Holzforschung* 56(2), 150-156. DOI: 10.1515/hf.2002.025
- Hu, W., Chen, S., Xu, Q., and Wang, H. (2011). “Solvent-free acetylation of bacterial cellulose under moderate conditions,” *Carbohydrate Polymers* 83, 1575-1581. DOI: 10.1016/j.carbpol.2010.10.016
- Ifuku, S., Nogi, M., Abe, K., Handa, K., Nakatsubo, F., and Yano, H. (2007). “Surface modification of bacterial cellulose nanofibers for property enhancement of optically transparent composites: Dependence on acetyl-group DS,” *Biomacromolecules* 8, 1973-1978. DOI: 10.1021/bm070113b
- Iwamoto, S., Nakagaito, A. N., Yano, H., and Nogi, M. (2005). “Optically transparent composites reinforced with plant fiber based nanofibers,” *Appl. Phys. A: Mater. Sci. Process.* 81(6), 1109-1112. DOI: 10.1007/s00339-005-3316-z
- Johansson, L.S., Tammelin, T., Campbell, J. M., Setälä, H., and Österberg, M. (2011). “Experimental evidence on medium driven cellulose surface adaptation demonstrated using nanofibrillated cellulose,” *Soft Matter*. 7, 10917-10924. DOI: 10.1039/c1sm06073b
- Jonoobi, M., Harun, J., Mathew, A. P., Hussein, B., and Oksman, K. (2010). “Preparation of cellulose nanofibers with hydrophobic surface characteristics,” *Cellulose* 17, 299-307. DOI: 10.1007/s10570-009-9387-9
- Jonoobi, M., Mathew, A. P., Abdi, M. M., Davoodi Makinejad, M., and Oksman, K. (2012). “A comparison of modified and unmodified cellulose nanofiber reinforced polylactic acid (PLA) prepared by twin screw extrusion,” *Journal of Polymer Environment* 20, 991-997. DOI: 10.1007/s10924-012-0503-9
- Kim, D. Y., Nishiyama, Y., and Kuga, S. (2002). “Surface acetylation of bacterial cellulose,” *Cellulose* 9(3-4), 361-367. DOI: 10.1023/A:1021140726936
- Lee, K. Y., and Bismarck, A. (2012). “Susceptibility of never-dried and freeze-dried bacterial cellulose towards esterification with organic acid,” *Cellulose* 19, 891-900. DOI: 10.1007/s10570-012-9680-x
- Lee, K. Y., Quero, F., Blaker, J. J., Hill, C. A. S., Eichhorn, S. J., and Bismarck, A. (2011). “Surface only modification of bacterial cellulose nanofibres with organic acids,” *Cellulose* 18(3), 595-605. DOI: 10.1007/s10570-011-9525-z
- Li, J., Zhang, L. P., Peng, F., Bian, J., Yuan, T. Q., Xu, F., and Sun, R. C. (2009a). “Microwave-assisted solvent-free acetylation of cellulose with acetic anhydride in the presence of iodine as a catalyst,” *Molecules* (14), 3551-3566. DOI: 10.3390/molecules14093551
- Li, X., Chen, S., Hu, W., Shi, S., Shen, W., Zhang, X., and Wang, H. (2009b). “In situ synthesis of CdS nanoparticles on bacterial cellulose nanofibers,” *Carbohydrate Polymers* 76, 509-512. DOI: 10.1016/j.carbpol.2008.11.014
- Li, W., Wu, L., Chen, D., Liu, C., and Sun, R. (2011). “Phthalylation of cellulose in ionic liquid,” *BioResources* 6(3), 2375-2385. DOI: 10.15376/biores.6.3.2375-2385
- Lin, N., Huang, J., Chang, P. R., Feng, J., and Yu, J. (2011). “Surface acetylation of cellulose nanocrystal and its reinforcing function in poly(lactic acid),” *Carbohydrate Polymers* 83, 1834-1842. DOI: 10.1016/j.carbpol.2010.10.047
- Liu, D., Zhong, T., Chang, P. R., Li, K., and Wu, Q. (2010). “Starch composites reinforced by bamboo cellulosic crystals,” *Bioresource Technology* 101, 2529-2536. DOI: 10.1016/j.biortech.2009.11.058

- Maneerung, T., Tokura, S., and Rujiravanit, R. (2008). "Impregnation of silver nanoparticles into bacterial cellulose for antimicrobial wound dressing," *Carbohydrate Polymers* 72, 43-51. DOI: 10.1016/j.carbpol.2007.07.025
- Miao, C., and Hamad, W. Y. (2013). "Cellulose reinforced polymer composites and nanocomposites: A critical review," *Cellulose* 20, 2221-2262. DOI: 10.1007/s10570-013-0007-3
- Missoum, K., Belgacem, M. N., Barnes, J. P., Brochier-Salon, M. C., and Bras, J. (2012). "Nanofibrillated cellulose surface grafting in ionic liquid," *Soft Matter* 8, 8338-8349. DOI: 10.1039/c2sm25691f
- Nishiyama, Y., Johnson, G. P., and French, A. (2012). "Diffraction from nonperiodic models of cellulose crystals," *Cellulose* 19, 319-336. DOI: 10.1007/s10570-012-9652-1
- Pääkkö, M., Ankerfors, M., Kosonen, H., Nykänen, A., Ahola, S., Osterberg, M., Ruokolainen, J., Laine, J., Larsson, P. T., Ikkala, O., and Lindström, T. (2007). "Enzymatic hydrolysis combined with mechanical shearing and high-pressure homogenization for nanoscale cellulose fibrils and strong gels," *Biomacromolecules* 8, 1934-1941. DOI: 10.1021/bm061215p
- Rebouillat, S., and Pla, F. (2013). "State of the art manufacturing and engineering of nanocellulose: A review of available data and industrial applications," *Journal of Biomaterials and Nanobiotechnology* 4, 165-188. DOI: 10.4236/jbnb.2013.42022
- Rodionova, G., Lenes, M., Eriksen, Ø., and Gregersen, Ø. (2011). "Surface chemical modification of microfibrillated cellulose: Improvement of barrier properties for packaging applications," *Cellulose* 18, 127-134. DOI: 10.1007/s10570-010-9474-y
- Saito, T., Nishiyama, Y., Putaux, J., Vignon, M., and Isogai, A. (2006). "Homogeneous suspensions of individualized microfibrils from TEMPO-catalyzed oxidation of native cellulose," *Biomacromolecules* 7, 1687-1691. DOI: 10.1021/bm060154s
- Sassi, J. F., and Chanzy, H. (1995). "Ultrastructural aspects of the acetylation of cellulose," *Cellulose* 2, 111-127. DOI: 10.1007/BF00816384
- Sassi, J. F., Tekely, P., and Chanzy, H. (2000). "Relative susceptibility of the I-alpha and I-beta phases of cellulose towards acetylation," *Cellulose* 7(2), 119-132. DOI: 10.1023/A:1009224008802
- Satchell, D. P. N (1963). "An outline of acylation," *Q. Rev. (London)* 17, 160-203. DOI: 10.1039/QR9631700160
- Satgé, C., Verneuil, B., Branland, P., Granet, R., Krausz, P., Rozier, J., and Petit, C. (2002). "Rapid homogeneous esterification of cellulose induced by microwave irradiation," *Carbohydrate Polymers* 49, 373-376. DOI: 10.1016/S0144-8617(02)00004-8
- Segal, L., Creely, J. J., Martin, A. E. Jr., and Conrad, C. M. (1959). "An empirical method for estimating the degree of crystallinity of native cellulose using X-Ray diffractometer," *Text. Res.* 29, 786-794. DOI: 10.1177/004051755902901003
- Šturcova, A., Davies, G. R., and Eichhorn, S. J. (2005). "Elastic modulus and stress-transfer properties of tunicate cellulose whiskers," *Biomacromolecules* 6(2), 1055-1061. DOI: 10.1021/bm049291k
- Sun, R., Sun, X. F., and Zhang, F. Y. (2001). "Succinoylation of wheat straw hemicelluloses in N,N-dimethylformamide/lithium chloride systems," *Polym. Int.* 50, 803-8011. DOI: 10.1002/pi.699

- Sun, X. F., Sun, R., and Sun, J. X. (2002). "Acetylation of rice straw with or without catalysts and its characterization as a natural sorbent in oil spill cleanup," *J. Agric. Food Chem.* 50(22), 6428-6433. DOI: 10.1021/jf020392o
- Tingaut, P., Zimmermann, T., and Lopez-Suevos, F. (2010). "Synthesis and characterization of bionanocomposites with tunable properties from poly(lactic acid) and acetylated microfibrillated cellulose," *Biomacromolecules* 11, 454-464. DOI: 10.1021/bm901186u
- Tosh, B., Saikia, C. N., and Dass, N. N. (2000). "Homogeneous esterification of cellulose in the lithium chloride N,N-dimethylacetamide solvent system: Effect of temperature and catalyst," *Carbohydrate Research* 327, 345-352. DOI: 10.1016/S0008-6215(00)00033-1
- Turbak, A. F., Snyder, F. W., and Sandberg, K. R. (1983). "Microfibrillated cellulose, a new cellulose product: properties, uses, and commercial potential," *J. Appl. Polym. Sci. Appl. Polym. Symp.* 37, 815-827. DOI: 10.1007/s00226-008-0194-5
- Yang, Z., Xu, S., Ma, X., and Wang, S. (2008). "Characterization and acetylation behaviour of bamboo pulp," *Wood Science and Technology* 42, 621-632. DOI: 10.1007/s00226-008-0194-5
- Yin, C., Li, J., Xu, Q., Peng, Q., Liu, Y., and Shen, X. (2007). "Chemical modification of cotton cellulose in supercritical carbon dioxide: Synthesis and characterization of cellulose carbamate," *Carbohydrate Polymers* 67(2), 147-154. DOI: 10.1016/j.carbpol.2006.05.010
- Zimmermann, T., Pohler, E., and Geiger, T. (2004). "Cellulose fibrils for polymer reinforcement," *Adv. Eng. Mater.* 6, 754-761. DOI: 10.1002/adem.200400097
- Zugenmaier, P. (2008). *Crystalline Cellulose and Derivatives: Characterization and Structures*, Springer, Berlin. DOI: 10.1007/978-3-540-73934-0
- Žepič, V., Fabjan, E. Š., Kasunič, M., Korošec, R. C., Hančič, A., Oven, P., Perše, L., and Poljanšek, I. (2014). "Morphological, thermal, and structural aspects of dried and redispersed nanofibrillated cellulose (NFC)," *Holzforschung* 68(6), 657-667. DOI:10.1515/hf-2013-0132

Article submitted: July 3, 2015; Peer review completed: August 24, 2015; Revised version received and accepted: October 1, 2015; Published: October 26, 2015.
DOI: 10.15376/biores.10.4.8148-8167